

Thermodynamics of $SU(3)$ Gauge Theory from Gradient Flow

Masayuki Asakawa,^{1,*} Tetsuo Hatsuda,^{2,3,†} Etsuko Itou,^{4,‡} Masakiyo Kitazawa,^{1,§} and Hiroshi Suzuki^{5,¶}
(FlowQCD Collaboration)

¹*Department of Physics, Osaka University, Toyonaka, Osaka 560-0043, Japan*

²*Theoretical Research Division, Nishina Center, RIKEN, Wako 351-0198, Japan*

³*Kavli IPMU (WPI), The University of Tokyo, Chiba 606-8502, Japan*

⁴*High Energy Accelerator Research Organisation (KEK), Tsukuba 305-0801, Japan*

⁵*Department of Physics, Kyushu University, 6-10-1 Hakozaki, Higashi-ku, Fukuoka, 812-8581, Japan*

A novel method to study the bulk thermodynamics in lattice gauge theory is proposed on the basis of the Yang–Mills gradient flow with a fictitious time t . The energy density ε and the pressure P of $SU(3)$ gauge theory at fixed temperature are calculated directly on $32^3 \times (6, 8, 10)$ lattices from the thermal average of the well-defined energy-momentum tensor $T_{\mu\nu}^R(x)$ obtained by the gradient flow. It is demonstrated that the continuum limit can be taken in a controlled manner from the t -dependence of the flowed data.

PACS numbers: 05.70.Ce; 11.10.Wx; 11.15.Ha

The symmetric energy momentum tensor (EMT), $T_{\mu\nu}$, which is the generator of the Poincaré transformations, is a fundamental operator in quantum field theory [1]. Since T_{00} , T_{i0} , and T_{ij} correspond to the energy density, the momentum density, and the momentum-flux density, respectively, the EMT and its correlation functions provide useful information on the bulk and transport properties at finite temperature (T). For example, the energy density ε and the pressure P are given by $\langle T_{00} \rangle$ and $\langle T_{11,22,33} \rangle$, respectively, with $\langle \cdot \rangle$ being the thermal average. Also, the shear viscosity η can be extracted from the two-point correlation, $\langle T_{12}(x)T_{12}(y) \rangle$. In quantum chromodynamics (QCD), these observables are particularly important in formulating the relativistic hydrodynamics for the quark-gluon plasma [2]. Therefore, high precision and non-perturbative evaluation of the n -point EMT correlations in lattice QCD is called for.

To calculate such correlations in numerical lattice simulations, we first need to define proper EMT on the lattice which is ultra-violet (UV) finite and is conserved in the continuum limit. Such a construction is not a trivial task due to the explicit breaking of the Poincaré invariance on the lattice. (See Refs. [3–6] for recent developments.) This is the reason why ε and P at finite T have been mainly studied by an indirect “integral method” without the explicit use of the EMT [7].

Recently, one of the present authors has shown that the proper EMT keeping all the nice features can be naturally constructed [8] on the basis of the Yang–Mills gradient flow [9–11]. (See also related works, Refs. [12–16].) In this Letter, we demonstrate, for the first time, that the thermal $SU(3)$ gauge theory can be studied by the direct lattice measurement of the proper EMT by considering ε and P as examples. The key idea is to represent the EMT in the continuum limit by UV-finite and local operators obtained from the gradient flow. Then, by taking the limit of small flow time and small lattice spacing in an appropriate way, as discussed later, accurate thermo-

dynamic observables are obtained with modest statistics.

Let us first recapitulate the basic idea of Ref. [8] in the continuum space-time. The Yang–Mills gradient flow is a deformation of the gauge configuration $A_\mu(x)$ along a fictitious Euclidean time t ; $\partial_t B_\mu(t, x) = D_\nu G_{\nu\mu}(t, x)$ with $B_\mu(t = 0, x) = A_\mu(x)$, where D_μ and $G_{\mu\nu}(t, x)$ are the covariant derivative and the field strength of the flowed gauge field $B_\mu(t, x)$, respectively. The color indices are suppressed for simplicity. A salient feature of the gradient flow is its UV finiteness: Any correlation functions of $B_{\mu_1}(t_1, x_1)$, $B_{\mu_2}(t_2, x_2)$, \dots for $t_i > 0$ are UV finite without the wave function renormalization if they are written in terms of the renormalized coupling [10]. This is owing to the fact that the diffusion in t naturally introduces a proper-time regulator of the form e^{-tp^2} , where p denotes a typical loop momentum. In particular, the correlation functions are free from UV divergences even at the equal-point, $(t_1, x_1) = (t_2, x_2) = \dots$ for positive t_i . For example, the following gauge-invariant local products of dimension 4 are UV finite for $t > 0$: $U_{\mu\nu}(t, x) \equiv G_{\mu\rho}(t, x)G_{\nu\rho}(t, x) - \frac{1}{4}\delta_{\mu\nu}G_{\rho\sigma}(t, x)G_{\rho\sigma}(t, x)$ and $E(t, x) \equiv \frac{1}{4}G_{\mu\nu}(t, x)G_{\mu\nu}(t, x)$.

For $t \rightarrow 0_+$, local products of flowed fields can be expanded in terms of four-dimensional renormalized local operators with increasing dimensions [10]: The expansion coefficients are governed by the renormalization group equation and their small t behavior can be calculated by perturbation theory thanks to the asymptotic freedom. For the operators mentioned above, we have [8, 17]

$$U_{\mu\nu}(t, x) = \alpha_U(t) \left[T_{\mu\nu}^R(x) - \frac{1}{4}\delta_{\mu\nu}T_{\rho\rho}^R(x) \right] + O(t), \quad (1)$$

$$E(t, x) = \langle E(t, x) \rangle_0 + \alpha_E(t)T_{\rho\rho}^R(x) + O(t), \quad (2)$$

where $\langle \cdot \rangle_0$ is vacuum expectation value and $T_{\mu\nu}^R(x)$ is the correctly-normalized conserved EMT with its vacuum expectation value subtracted. Abbreviated are the contributions from the operators of dimension 6 or higher,

which are suppressed for small t .

Combining relations Eqs. (1) and (2), we have

$$T_{\mu\nu}^R(x) = \lim_{t \rightarrow 0} \left\{ \frac{1}{\alpha_U(t)} U_{\mu\nu}(t, x) + \frac{\delta_{\mu\nu}}{4\alpha_E(t)} [E(t, x) - \langle E(t, x) \rangle_0] \right\}, \quad (3)$$

where the perturbative coefficients are found to be [8]

$$\alpha_U(t) = \bar{g}(1/\sqrt{8t})^2 \left[1 + 2b_0 \bar{s}_1 \bar{g}(1/\sqrt{8t})^2 + O(\bar{g}^4) \right], \quad (4)$$

$$\alpha_E(t) = \frac{1}{2b_0} \left[1 + 2b_0 \bar{s}_2 \bar{g}(1/\sqrt{8t})^2 + O(\bar{g}^4) \right]. \quad (5)$$

Here $\bar{g}(q)$ denotes the running gauge coupling in the $\overline{\text{MS}}$ scheme with the choice, $q = 1/\sqrt{8t}$, and $\bar{s}_1 = \frac{7}{22} + \frac{1}{2}\gamma_E - \ln 2 \simeq -0.08635752993$, $\bar{s}_2 = \frac{21}{44} - \frac{b_1}{2b_0^2} = \frac{27}{484} \simeq 0.05578512397$, with $b_0 = \frac{1}{(4\pi)^2} \frac{11}{3} N_c$, $b_1 = \frac{1}{(4\pi)^4} \frac{34}{3} N_c^2$, and $N_c = 3$. Note that a non-perturbative determination of $\alpha_{U,E}(t)$ is also proposed recently [17].

The formula Eq. (3) indicates that $T_{\mu\nu}^R(x)$ can be obtained by the small t limit of the gauge-invariant local operators defined through the gradient flow. There are two important observations: (i) The right-hand side of Eq. (3) is independent of the regularization because of its UV finiteness, so that one can take, e.g. the lattice regularization scheme; (ii) since flowed fields at $t > 0$ depend on the fundamental fields at $t = 0$ in the space-time region of radius $\simeq \sqrt{8t}$, the statistical noise in calculating the right hand side of Eq. (3) is suppressed for finite t .

Our procedure to calculate the EMT on the lattice has the following four steps:

Step 1: Generate gauge configurations at $t = 0$ on a space-time lattice with the lattice spacing a and the lattice size $N_s^3 \times N_\tau$.

Step 2: Solve the gradient flow for each configuration to obtain the flowed link variables in the fiducial window, $a \ll \sqrt{8t} \ll R$. Here, R is an infrared cutoff scale such as $\Lambda_{\text{QCD}}^{-1}$ or $T^{-1} = N_\tau a$. The first (second) inequality is necessary to suppress finite a corrections (non-perturbative corrections and finite volume corrections).

Step 3: Construct $U_{\mu\nu}(t, x)$ and $E(t, x)$ in Eqs. (1) and (2) in terms of the flowed link variables and average over the gauge configurations at each t .

Step 4: Carry out an extrapolation toward $(a, t) = (0, 0)$, first $a \rightarrow 0$ and then $t \rightarrow 0$ under the condition in **Step 2**.

The thermodynamic quantities are obtained from the diagonal elements of the EMT: A combination of ε and P called the interaction measure Δ is related to the trace of the EMT (the trace anomaly):

$$\Delta = \varepsilon - 3P = -\langle T_{\mu\mu}^R(x) \rangle. \quad (6)$$

Also, the entropy density s at zero chemical potential

N_τ	6	8	10	T/T_c
	6.20	6.40	6.56	1.65
β	6.02	6.20	6.36	1.24
	5.89	6.06	6.20	0.99

TABLE I: Values of β and N_τ for each temperature.

reads

$$sT = \varepsilon + P = -\langle T_{00}^R(x) \rangle + \frac{1}{3} \sum_{i=1,2,3} \langle T_{ii}^R(x) \rangle. \quad (7)$$

To demonstrate that the above four Steps can be indeed pursued, we consider the $SU(3)$ gauge theory defined on a four-dimensional Euclidean lattice, whose thermodynamics has been extensively studied by the integral method [18–21]. For simplicity, we consider the Wilson plaquette gauge action under the periodic boundary condition on $N_s^3 \times N_\tau = 32^3 \times (6, 8, 10)$ lattices with several different $\beta = 6/g_0^2$ (g_0 being the bare coupling constant). Gauge configurations are generated by the pseudo-heatbath algorithm with the over-relaxation, mixed in the ratio of 1 : 5. We call one pseudo-heatbath update sweep plus five over-relaxation sweeps as a ‘‘Sweep’’. To eliminate the autocorrelation, we take 200–500 Sweeps between measurements. The number of gauge configurations for the measurements at finite T is 300. Statistical errors are estimated by the jackknife method.

To relate T/T_c and corresponding β for each N_τ , we first use the relation between a/r_0 (r_0 is the Sommer scale) and β given by the ALPHA Collaboration [22]. The resultant values of $Tr_0 = [N_\tau(a/r_0)]^{-1}$ are then converted to T/T_c by using the result at $\beta = 6.20$ in Ref. [18]. Nine combinations of (N_τ, β) and corresponding T/T_c obtained by this procedure are shown in Table I.

The gradient flow in the t -direction is obtained by solving the ordinary first-order differential equation. We utilize the modified second-order Runge–Kutta method in which the error per step ($t \rightarrow t + \epsilon$) is $O(\epsilon^3)$. We take $\epsilon = 0.025$, and confirm that the accumulation errors are sufficiently smaller than the statistical errors.

To extract the EMT from Eq. (3), we measure $G_{\mu\rho}^a(t, x)G_{\nu\rho}^a(t, x)$ written in terms of the clover leaf representation on the lattice. To subtract out the $T = 0$ contribution, $\langle E(t, x) \rangle_0$, we carry out simulations on a 32^4 lattice for each β in Table I. Note that this vacuum subtraction is required for the trace anomaly Δ , but not for the entropy density s . For \bar{g} in $\alpha_U(t)$ and $\alpha_E(t)$ in Eqs. (4) and (5), we use the four-loop running coupling with the scale parameter determined by the ALPHA Collaboration, $\Lambda_{\overline{\text{MS}}} = 0.602(48)/r_0$ [23]. We confirmed the previous finding [9] that the lattice data of $t^2 \langle E(t, x) \rangle_0$ in the fiducial window matches quite well with its perturbative estimate in the continuum,

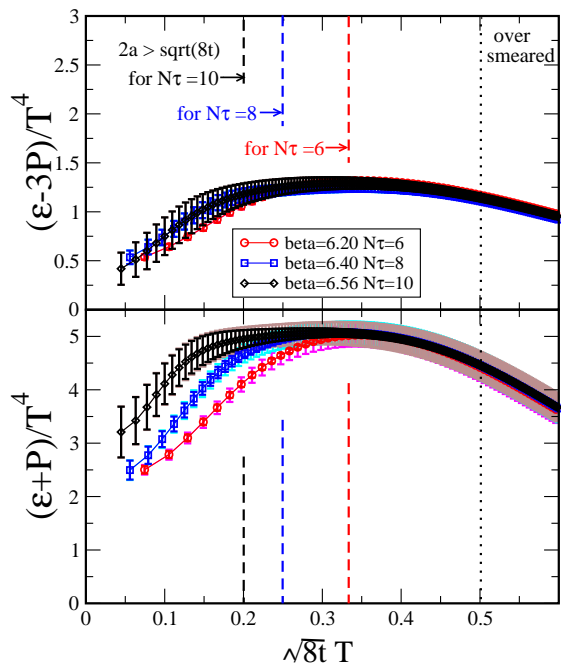


FIG. 1: Flow time dependence of the dimensionless interaction measure (top panel) and the dimensionless entropy density (bottom panel) for different lattice spacings at fixed $T/T_c = 1.65$. The circles (red) the squares (blue), and the diamonds (black) correspond to $N_\tau = 6, 8$, and 10 , respectively. The bold error bars denote the statistical errors, while the thin error bars (brown, cyan, and magenta) include both statistical and systematic errors.

$t^2 \langle E(t, x) \rangle_0 \simeq 3\bar{g}^2 / (4\pi)^2 [1 + 1.0978\bar{g}(1/\sqrt{8t})^2 / (4\pi)]$ with the four-loop running coupling and the above $\Lambda_{\overline{\text{MS}}}$.

Shown in Fig. 1 is our results for the dimensionless interaction measure ($\Delta/T^4 = (\varepsilon - 3P)/T^4$) and the dimensionless entropy density ($s/T^3 = (\varepsilon + P)/T^4$) at $T = 1.65T_c$ as a function of the dimensionless flow parameter $\sqrt{8t}T$. The bold bars denote the statistical errors, while the thin (light color) bars show the statistical and systematic errors including the uncertainty of $\Lambda_{\overline{\text{MS}}}$. In the small t region, the statistical error is dominant for both Δ/T^4 and s/T^3 , while in the large t region the systematic error from $\Lambda_{\overline{\text{MS}}}$ becomes significant for s/T^3 . For instance, the statistical (systematic) errors of the data for $N_\tau = 8$ are 2.5% (0.11%) for Δ/T^4 and 0.83% (4.4%) for s/T^3 at $\sqrt{8t}T = 0.40$.

The fiducial window discussed in **Step 2** is indicated by the dashed lines in Fig. 1. The lower limit, beyond which the lattice discretization error grows, is set to be $\sqrt{8t_{\min}} = 2a$, where we consider the size $2a$ of our clover leaf operator. The upper limit, beyond which the smearing by the gradient flow exceeds the temporal lattice size, is set to be $\sqrt{8t_{\max}} = 1/(2T) = N_\tau a/2$.

The data in Fig. 1 show, within the error bars, that (i) the plateau appears inside the preset fiducial win-

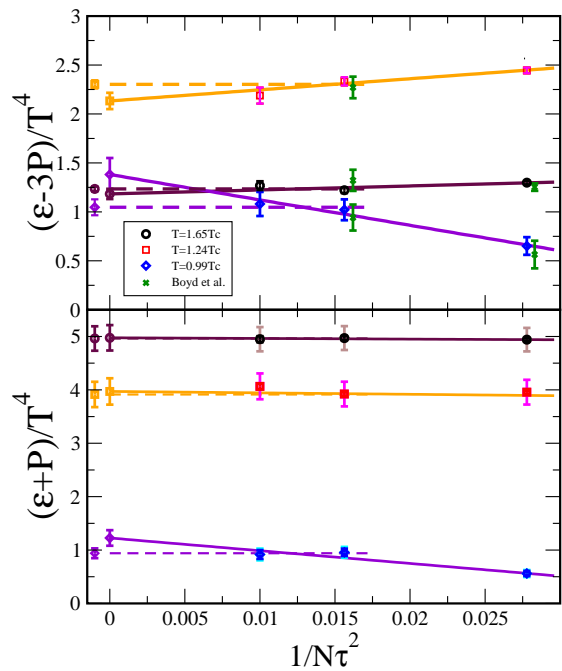


FIG. 2: Continuum extrapolation of the thermodynamic quantities for $T/T_c = 1.65, 1.24$, and 0.99 . Solid lines and dashed lines correspond to the three-point linear fit and two-point constant fit as a function of $1/N_\tau^2$, respectively. Extrapolated values of the former (latter) are shown at $1/N_\tau^2 = 0$ ($1/N_\tau^2 = -0.001$). The cross symbols in the top panel are the data of Ref. [18] with the same lattice setup.

dow ($2/N_\tau < \sqrt{8t}T < 1/2$) for each N_τ , and (ii) the plateau extends to the smaller t region as N_τ increases or equivalently as a decreases. Similar plateaus as in Fig. 1 also appear inside the fiducial window for other temperatures, $T/T_c = 1.24$ and 0.99 , with comparable error bars. These features imply that the double extrapolation $(a, t) \rightarrow (0, 0)$ in **Step 4** is indeed doable.

Our lattice results at fixed T with three different lattice spacings allow us to take the continuum limit. First, we pick up a flow time $\sqrt{8t}T = 0.40$ which is in the middle of the fiducial window. Then we extract Δ/T^4 and s/T^3 for each set of N_τ and β . We have checked that different choices of t do not change the final results within the error bar as long as it is in the plateau region. In Fig. 2, resultant values taking into account the statistical errors (bold error bars) and the statistical plus systematic errors (thin error bars) are shown. The lattice data for Δ/T^4 with the same lattice setup at $N_\tau = 6$ and 8 in Ref. [18] are also shown by the cross (green) symbols in the top panel; the statistical error of our result on $32^3 \times 8$ lattice for $\beta = 6.4$ ($\beta = 6.2$) is about 3.33 (2.69) times smaller than the one in Ref. [18] obtained on the same lattice. In this way, our results with 300 gauge configurations have substantially smaller error bars at these points.

The horizontal axis of Fig. 2, $1/N_\tau^2$, is a variable suited

for making continuum extrapolation of the thermodynamic quantities [18]. We consider two extrapolation: A linear fit with the data at $N_\tau = 6, 8,$ and 10 (the solid lines in Fig. 2), and a constant fit with the data at $N_\tau = 8$ and 10 (the dashed lines in Fig. 2). In both fits, the correlation between the errors due to the common systematic error from $\Lambda_{\overline{\text{MS}}}$ is taken into account. The former fit is used to determine the central value in the continuum limit whose error is within $\pm 12\%$ even at our lowest temperature. The latter is used to estimate the systematic error from the scaling violation whose typical size is $\pm 5\%$ at high temperature and $\pm 25\%$ at low temperature.

We have analyzed various systematic errors; the perturbative expansion of $\alpha_{U,E}(t)$, the running coupling \bar{g} , the scale parameter, and the continuum extrapolation. We found that the dominant errors in the present lattice setup are those from $\Lambda_{\overline{\text{MS}}}$ and the continuum extrapolation, which are included in Fig. 2. To reduce these systematic errors, finer lattices are quite helpful: They make the plateau in $\sqrt{8t}T$ wider by reducing the lower limit of the fiducial window, so that the continuum extrapolation becomes easier. We also note that our continuum extrapolation with fixed $N_s = 32$ would receive the finite volume effect especially for lower T [12]. Larger aspect ratio N_s/N_τ would be helpful to guarantee the thermodynamic limit. Moreover, the scale setting procedure could be improved to have better accuracy: Instead of the Sommer scale r_0 adopted in this Letter, more precise scale determination, e.g. by t_0 or ω_0 in the gradient flow approach [9, 14], will be useful.

Finally, we plot, in Fig. 3, the continuum limit of Δ/T^4 and s/T^3 obtained by the linear fit of the $N_\tau = 6, 8,$ and 10 data (the solid lines) in Fig. 2 for $T/T_c = 1.65, 1.24,$ and 0.99 . For comparison, the results of Ref. [18, 19, 21] obtained by the integral method are shown by the magenta, green, and blue data in Fig. 3. The results of the two different approaches are consistent with each other within the statistical error.

In this Letter, we have proposed and demonstrated a novel way to study thermal $SU(3)$ gauge theory on the lattice. The key ingredient is the conserved and UV-finite energy-momentum tensor $T_{\mu\nu}^R(x)$ defined from the UV-finite operators ($U_{\mu\nu}(t, x)$ and $E(t, x)$) obtained from the Yang-Mills gradient flow with the matching coefficients ($\alpha_{U,E}(t)$) [8]. From the simulations on $32^3 \times (6, 8, 10)$ lattices with modest statistics (300 gauge configurations), we found that the dimensionless interaction measure and entropy density, $(\varepsilon - 3P)/T^4$ and $(\varepsilon + P)/T^4$, show plateau structure inside the fiducial window ($2/N_\tau < \sqrt{8t}T < 1/2$) with small statistical errors, so that the double extrapolation $(a, t) \rightarrow (0, 0)$ can be taken appropriately for given T .

Major advantages of the gradient flow applied to the lattice thermodynamics are as follows: (i) One can simulate ε and P independently at any fixed T through the

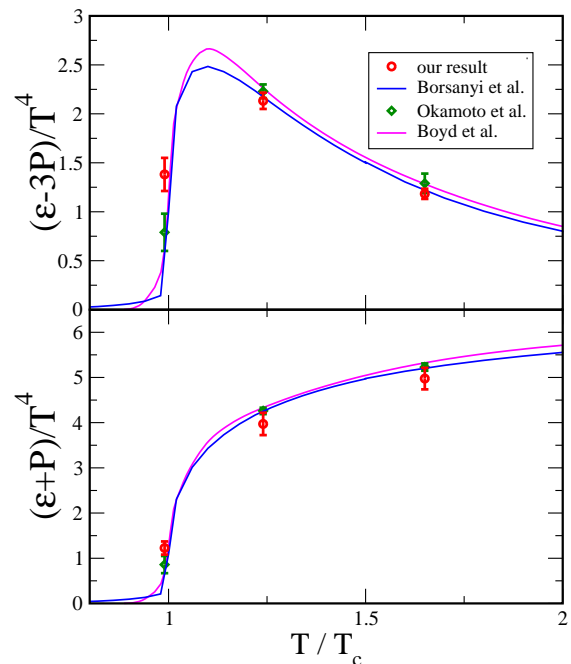


FIG. 3: Continuum limit of the interaction measure and entropy density obtained by the gradient flow for $T/T_c = 1.65, 1.24,$ and 0.99 with 300 gauge configurations. The magenta, green, and blue data are the results of the integral method according to Ref. [18, 19, 21], respectively

direct measurement of the well-defined EMT. There is no need of integration by β or T , which requires a boundary condition and the numerical interpolation. (ii) There is no need of constant subtraction in entropy density s . The interaction measure Δ needs one subtraction of its $T = 0$ value, which is obtained by the accurate measurement of $t^2 \langle E(t, x) \rangle_0$ or by its perturbative evaluation at small t . (iii) The statistical noise is substantially reduced at finite flow time $t > 0$ due to the effective smearing of the operators with the radius $\simeq \sqrt{8t}$, so that the extrapolation of the results back to $t = 0$ is well under control.

Although we studied only the thermal average of EMT in this Letter, there is no conceptual difficulties in applying our method to $n(\geq 2)$ -point EMT correlations [8]. This opens the door to investigate transport coefficients (such as shear and bulk viscosities), fluctuation observables in the hot plasma, glueballs at zero and finite temperatures. Here we note that there is no difficulty in measuring thermodynamic quantities even at extremely high temperature in this method since no temperature integration is necessary. It is also an interesting direction to study the dilation mode or the a -function of (nearly) conformal theory [24, 25] using the present method. Furthermore, including fermions in the present framework extends the scope even further [26]. Some of these issues as well as the simulations with finer lattice with larger volume are already started and will be reported

elsewhere.

We would like to thank S. Aoki, F. Karsch, M. Lüscher, and H. Nagatani for useful discussions and comments. We are also grateful to H. Matsufuru for his help of the code development. Numerical simulation was carried out on NEC SX-8R and SX-9 at RCNP, Osaka University, and Hitachi SR16000 at KEK under its Large-Scale Simulation Program (Nos. T12-04 and 13/14-20). M. A., M. K., and H. S. are supported in part by a Grant-in-Aid for Scientific Researches 23540307, 25800148, and 23540330, respectively. E. I. is supported in part by Strategic Programs for Innovative Research (SPIRE) Field 5. T. H. is supported by RIKEN iTHES Project.

* Electronic address: yuki@phys.sci.osaka-u.ac.jp

† Electronic address: thatsuda@riken.jp

‡ Electronic address: eitou@post.kek.jp

§ Electronic address: kitazawa@phys.sci.osaka-u.ac.jp

¶ Electronic address: hsuzuki@phys.kyushu-u.ac.jp

- [1] S. Caracciolo, G. Curci, P. Menotti and A. Pelissetto, *Annals Phys.* **197**, 119 (1990).
- [2] Reviewed in, P. Romatschke, *Int. J. Mod. Phys. E* **19**, 1 (2010) [arXiv:0902.3663 [hep-ph]].
- [3] L. Giusti and H. B. Meyer, *JHEP* **1301**, 140 (2013) [arXiv:1211.6669 [hep-lat]].
- [4] D. Robaina and H. B. Meyer, arXiv:1310.6075 [hep-lat].
- [5] L. Giusti and H. B. Meyer, arXiv:1310.7818 [hep-lat].
- [6] L. Giusti and M. Pepe, arXiv:1311.1012 [hep-lat].
- [7] Reviewed in, M. P. Lombardo, *PoS LATTICE* **2012**, 016 (2012) [arXiv:1301.7324 [hep-lat]].
- [8] H. Suzuki, *PTEP* **2013**, no. 8, 083B03 (2013) [Erratum: *PTEP* **2015**, no. 7, 079201 (2015)] [arXiv:1304.0533 [hep-lat]].
- [9] M. Lüscher, *JHEP* **1008**, 071 (2010) [arXiv:1006.4518 [hep-lat]].
- [10] M. Lüscher and P. Weisz, *JHEP* **1102**, 051 (2011) [arXiv:1101.0963 [hep-th]].
- [11] Reviewed in, M. Lüscher, arXiv:1308.5598 [hep-lat].
- [12] S. Borsanyi, S. Dürr, Z. Fodor, C. Hoelbling, S. D. Katz, S. Krieg, T. Kurth and L. Lellouch *et al.*, *JHEP* **1209**, 010 (2012) [arXiv:1203.4469 [hep-lat]].
- [13] S. Borsanyi, S. Dürr, Z. Fodor, S. D. Katz, S. Krieg, T. Kurth, S. Magers and A. Schäfer *et al.*, arXiv:1205.0781 [hep-lat].
- [14] Z. Fodor, K. Holland, J. Kuti, D. Nogradi and C. H. Wong, *JHEP* **1211**, 007 (2012) [arXiv:1208.1051 [hep-lat]].
- [15] P. Fritzsche and A. Ramos, *JHEP* **1310**, 008 (2013) [arXiv:1301.4388 [hep-lat]].
- [16] M. Lüscher, *JHEP* **1304**, 123 (2013) [arXiv:1302.5246 [hep-lat]].
- [17] L. Del Debbio, A. Patella and A. Rago, *JHEP* **1311**, 212 (2013) [arXiv:1306.1173 [hep-th]].
- [18] G. Boyd, J. Engels, F. Karsch, E. Laermann, C. Legeland, M. Lutgemeier and B. Petersson, *Nucl. Phys. B* **469**, 419 (1996) [hep-lat/9602007].
- [19] M. Okamoto *et al.* [CP-PACS Collaboration], *Phys. Rev. D* **60**, 094510 (1999) [hep-lat/9905005]; Y. Namekawa *et al.* [CP-PACS Collaboration], *Phys. Rev. D* **64**, 074507 (2001).
- [20] T. Umeda, S. Ejiri, S. Aoki, T. Hatsuda, K. Kanaya, Y. Maezawa and H. Ohno, *Phys. Rev. D* **79**, 051501 (2009) [arXiv:0809.2842 [hep-lat]].
- [21] S. Borsanyi, G. Endrodi, Z. Fodor, S. D. Katz and K. K. Szabo, *JHEP* **1207**, 056 (2012) [arXiv:1204.6184 [hep-lat]].
- [22] M. Guagnelli *et al.* [ALPHA Collaboration], *Nucl. Phys. B* **535**, 389 (1998) [hep-lat/9806005].
- [23] S. Capitani *et al.* [ALPHA Collaboration], *Nucl. Phys. B* **544**, 669 (1999) [hep-lat/9810063].
- [24] T. Appelquist and Y. Bai, *Phys. Rev. D* **82**, 071701 (2010) [arXiv:1006.4375 [hep-ph]].
- [25] J. I. Latorre and H. Osborn, *Nucl. Phys. B* **511**, 737 (1998) [hep-th/9703196].
- [26] H. Makino and H. Suzuki, *PTEP* **2014**, no. 6, 063B02 (2014) [Erratum: *PTEP* **2015**, no. 7, 079202 (2015)] [arXiv:1403.4772 [hep-lat]].